The 6th International Conference on
Structural Health Monitoring of Intelligent Infrastructure
Hong Kong | 9-11 December 2013

RESEARCH ON THE THICKNESS OF FRAME BEAM GRIPPING GFRP ANCHOR BOLT WITH BUILT-IN FIBER BRAGG GRATING SENSOR

Guowei Li [1,2], Liang Yu [1], Jianhua Yin [3] and Jiantao Wu [2]
1. Key Laboratory of Ministry of Education for Geotechnique and Embankment Engineering, Hohai University, Nanjing, Jiangsu 210098, China. Email: lgwnj@163.com
2. Highway and Railway Engineering Institute, Hohai University, Nanjing, Jiangsu 210098, China.
3. Hong Kong Polytechnic University, Hung Hom, Kowloon, Hong Kong, China.

ABSTRACT

Fiber reinforced polymer (FRP) is a new composite material with excellent mechanical properties and corrosion resistance. It is a significant way to solve the durability problem of anchor bolt by substituting this polymer for steel bars. In this study, an anchor-bar-structure specimen is firstly fabricated using glass fiber reinforced polymer (GFRP) bars with fiber grating installed inside. Hollow hydraulic jack is then employed to load on the specimen and its responding strain is monitored by grating sensing technology. Based on these, the optimum thickness of frame beam gripping the larger diameter sand coated GFRP bolt under anchoring conditions is studied thoroughly. The test result shows that the tensile force and average bond strength of large-diameter (26 mm) GFRP rebar in this study has reached the design strength of ribbed steel with the same diameter; and the optimum thickness of frame beam ranges from 30 to 40 cm. In addition, it is found that sustained loads can lead to continuous degradation of the bar body interface-bond state, and the degradation keeps developing towards the deeper part during the loading progress. More attention should be paid to the bond behavior deterioration at interface in the future, because it can significantly affect the durability of frame beam gripping function and the magnitude of prestressed load.

KEY WORDS

Geotechnical engineering, anchor rod, durability, glass fiber reinforced polymer (GFRP), fiber bragg grating (FBG), bond behavior.

INTRODUCTION

The use of ground anchors has been a common practice in civil engineering. Ground anchors function as temporary or permanent structural members to ensure the stability of various structural systems. In general terms, a grouted anchor is a bar that is inserted and grouted into a hole drilled in rock/concrete. Steel strands and wires have been used as anchor tendons for many years, but in certain aggressive environments, corrosion of steel tendons leads to durability problems (Koch *et al.* 2005). In mainland China, anchor bolt structures were widely used for engineering reinforcement in 1960s. The problem of low durability in reinforced structures exists also. (Zeng *et al.* 2004). More recently, fiber-reinforced polymer (FRP) rods have been introduced in the market as tendons for prestressed concrete structures and prestressed ground anchors. (Zhang *et al.* 2001)

FRP mainly based on thermoset polymers (vinylester) and glass or carbon fibers, are being used in infrastructures exposed to harsh environments (Gilbert Nkurunziza *et al.* 2005). FRP bar is used due to its high stiffness/weight ratio, high strength/weight ratio, corrosion resistance, and ease in fabrication (Chu and Karbhari, 2005; Karbhari *et al.* 2003.). One of the potential solutions to steel - corrosion-related problems is the usage of FRP as a replacement for traditional steel bars.

The bond behavior of FRP is different from that of the steel embedded in concrete under the loading because of their different material characteristics. The steel anchor bolt does not need any grip measures for the frame beam of reinforced structures in civil slope engineering to satisfy the requirement of design. Otherwise, if the FRP anchor bolts need the extra unique method to grip for the frame beam, it would be too complicated for construction wide application.

In the past few decades, the durability of the GFRP materials is recognized as the most critical issue of research. Extensive studies were conducted on the durability of the GFRP material in 1990s (Yi Chen *et al.* 2007. A. S. M. Kamal *et al.* 2011. Saleh Alsayed *et al.* 2012), including the behavior of GFRP materials and the bond characteristics of GFRP bars in concrete. (Masmoudi *et al.* 2011; Zhou *et al.* 2011; Alves *et al.* 2011). In addition, the anchor bolt often adopted the larger geometric size bar (more than 25 mm of diameter) for the construction reinforcement (Zhu *et al.* 2011). Most of studies on GFRP bar reported in literature were conducted on smaller size of specimens. The diameter is usually less than 20 mm. Previous research results revealed that larger diameter GFRP bar has the shorter bonding strength than the smaller size under the same condition (Alves *et al.* 2011; Nanni *et al.* 1995; Benmokrane *et al.* 1996). As the presence of the difference of the bonding strength for different size GFRP bar, the behavior of larger size GFRP bar is still not well understood and further research in this aspect is required.

In fact, if the larger diameter GFRP bar can be griped well by the concrete frame beam individually like that of steel bar which can undertake the pull load designed in reinforced structure of civil engineering, that is perfect method for GFRP bar bolt application. The main objectives of this paper are to examine the bond behavior of larger diameter GFRP bar embedded in concrete and to determine the optimized thickness of frame beam.

EXPERIMENTAL PROGRAMS

GFRP Sand-Coated Bars

The GFRP bars used in this study are made of epoxy resin and glass fibers. As shown in Figure 1, the reinforcement materials used in this test is the glass fiber composites with diameter of 26mm produced by Zhongshan Pulwell Composites Co. Ltd. in Guangdong Province China, the basic body is a thermosetting epoxy resin, and the contents of each component (by weight) are: resin for 17.3 %; glass fiber for 75.7%; fine sand for 7%. The mechanical test of the reinforcement material was carried out. The details for physical and mechanical properties of FRP bars used in this study are listed in Tables 1.

Figure 1. Photos of GFRP rebar

Table 1. Physical and mechanical properties of FRP rebars

Average diameter (mm)	Density (g/cm^3)	Content (weight ratio %)			Ultimate tensile load (kN)	Ultimate tensile strength (MPa)	Modulus of elasticity (MPa)
		Glass	Resin	Fine sand			
26.17	2.07	75.7	17.3	7	458.7	852.79	49.96

Test Devices and Specimen

Griping the GFRP bar with a device which could undertake the tensile load for any measurement of mechanic properties is a key technique. In this study the seamless steel pipe was used to grip the GFRP bar by filling the binding agent which could expand by itself to create compressive stress gradually (Li *et al.* 2013).

Loading system for the test consisted of hollow jack, bearing plate, load cell, loading pads, and bed plates which could move with the bearing plate during the hollow jack loading, as shown in Figure 2. The bearing plates could fix the specimen at the suitable position by locking the pipe end of griping pipe in the groove located on the plate, and the optic fiber wires for monitoring could be connected to outside by crossing the U gap, as shown in Figure 3. When the piston of the hollow jack pushes the bearing plate to move, it could create the space between the bearing plate and the shell of hollow jack, and then loading pads were put in the gap to keep the space constant. As shown in Figure 4, corresponding pads were used at different loading stages. The surfaces of pad are smooth enough to keep the load distributing on the bearing plate uniformly.

The main advantage of this setup is that it can produce an enough tensile stress reached to 70% of its ultimate tensile strength for the large diameter GFRP bar at the condition of constant deformation. Furthermore, it does not require a large counter weight and large space and it is easy to operate.

Dimensions of the GFRP bar were 26 mm in diameter, 500mm in free part length, and 300 mm in anchorage length. This dimension is similar to the most common soil nails or anchor bolts used in practical field. The properties of concrete cube of soil nail element were listed in Table 2.

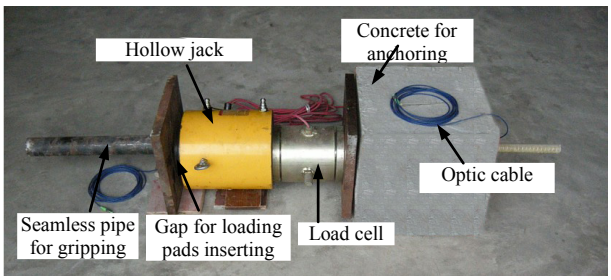

Figure 2. Physical map of loading equipment

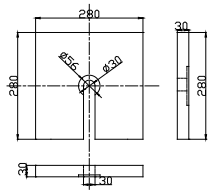

Figure 3. Bearing plate

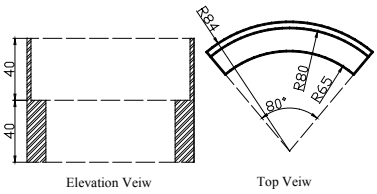

Figure 4. Loading pads

Table 2. Parameters of concete cube of frame beam

Item	Quantity or ratio
Cement (42.5R)	306.29kg/m^3
Natural sand	612.57kg/m^3
Gravel	1072.00kg/m^3
Water	153.14kg/m^3
cement /sand /Gravel/Water ratio	1 : 2 : 3.5 : 0.5
Standard cube specimen strength(150mm×150mm×150mm）	34.50MPa
Density in condensation state	2144kg/m^3

Strain Monitor Devices

For the measurement of occurred strain along the GFRP bar during loading process, a total of five fiber Bragg grating (FBG) sensors were mounted on the GFRP bar surface and locations of the five FBG sensors (in the anchorage part) were 40, 110, 180, and 250 mm to the bar tip, with one additional FBG sensor mounted on the free bar part (550 mm to the bar tip). Optic fiber Bragg grating (FBG) sensors were installed along the FRP bar body, as shown in Figure 5. FBG sensor is more sensitive to the occurred small deformation. The installation method of optical fiber sensors is a key procedure to reflect the real deformation of structures. In the present test, a 2 mm wide slot was created on the GFRP bar surface. The FBG sensor part was embedded in the slot and initially fixed with instant glue at the two ends. Then epoxy resin was used to cover the whole sensor part. Normally after 2-3 hours, the FBG sensor would be encapsulated in the slot and used to reflect the strain change. Since FBG sensor is a flexible material and not sensitive to compression, so that all FBG sensors were maintained in slightly tension effect before placing into slots of GFRP bar surface. Figure 6 shows the FBG sensor embedded condition in the GFRP bar slot and fully covered with epoxy resin.

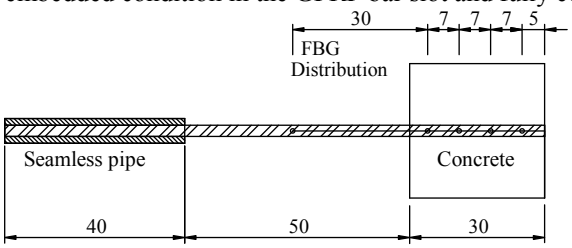

Figure 5. Schematic diagram of specimen(unit: cm)

Figure 6. GFRP bar Built-in FBG

The FBG sensor reflects the magnitude of optical wavelength shift associated with external deformation and temperature change. The obtained optical wavelength is linear proportional to the strain or temperature change as below:

$$\Delta\lambda_B / \lambda_B = c_\varepsilon \cdot \Delta\varepsilon + c_T \cdot \Delta T \quad (1)$$

Where λ_B and $\Delta\lambda_B$ are the measured central wavelength and the corresponding wavelength change; $\Delta\varepsilon$ and ΔT are the external strain and temperature change, c_ε and c_T are constant coefficients related to strain and temperature, respectively. Calibration test results indicate that these coefficient values for the present FBG strain and temperature sensors are 0.78×10-6 $\mu\varepsilon^{-1}$ and 6.67×10-6 $^oC^{-1}$, respectively.

In the present test, the strain caused from the temperature variation of surrounding was not considered because the duration of time for one stage load added on the specimen is not more than 10 minutes in which the temperature variation is too small to influence strain of FBG sensor. Optical Sensing Interrogator SM 125 was used to collect strain data. The data acquisition frequency was 1 Hz.

Loading Procedures on the Specimen

In the present test, the concrete was cured 28 days after grouting and used for pullout test. A step loading method was employed to apply pullout force on the GFRP bar head. Loading increment was 30 kN and maintained 10 minutes for each loading step. The ultimate pullout force applied at the GFRP bar head was 210 kN. During the pullout test process, all pullout force results and strain data were collected by load cell and optical fiber sensors, respectively.

TEST RESULTS AND ANALYSIS

Ultimate Bond Strength

When pulling out the GFRP bar from the concrete, the ultimate pullout force was 240 kN which was 53.2% of ultimate tensile strength of GFRP bar. The GFRP bar was not destroyed obviously when the anchor concrete cracked. This value of ultimate pullout force for GFRP bar in concrete is more than the pullout force of steel bolt required in design plan.

The ultimate bond strength between GFRP bar and concrete was 9.24 MPa obtained from the equation (2).

$$\tau_{ave} = \frac{P_u}{\pi d L} \quad (2)$$

Where, τ_{ave} is average bond strength between anchor bolt and concrete (MPa). P_u is ultimate bear load of anchor bolt (kN). L is the length of bolt anchored in the concrete (m). d is the diameter of GFRP bar.

The maximum bond strength value of ribbed steel anchored in concrete is smaller than the value of 2.70MPa which is regulated by China Code (GB50330—2002). The test result reveals that GFRP bar anchored in concrete possess enough bond strength for the pull force required in designed plan. Table 3 lists the values of bond strength of steel bolt in concrete regulated by the criterion of China.

Table 3. Steel bolt bond strength regulated in China criterion

Strength level of mortar	M25	M30	M35
Bond strength of interface between ribbed steel bar and mortar (MPa)	2.10	2.40	2.70

The Maximum Value of Bond Stress between GFRP Bar and Concrete

Figure 7 displays the strains at different depth along the GFRP bar under the scheduled load level. It can be seen that the strain decreases with the depth increasing under all loading level. In general, the bigger load causes the bigger decreasing rate. At the smaller depth the bigger decreasing rate was observed.

Figure 8 displays the strain at a certain depth under different load level. The strain increases with the load increasing at all locations of bar body. At the location -26 cm of GFRP bar, free state, the strain almost increases linearly with loading level. In terms of the part from 0 - 30 cm of the bar which was anchored in the concrete, the strain increases nonlinearly with loading level. The strain increasing rates of the GFRP bar are found to decrease with the increase of depth.

The model presented by YOU Chun′an (2000) can be used to describe the distribution of the axial force and boundary shear stress along the anchor bolt grouted wholly with concrete.

$$N = P\exp(az^2) \tag{4}$$

$$\tau = -\frac{azP}{\pi r}\exp(az^2) \tag{5}$$

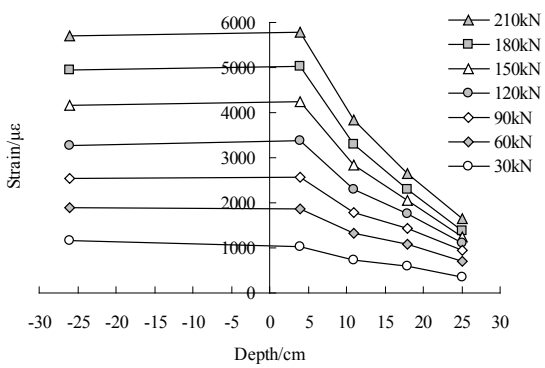

Figure 7. Strain distribution curves under different loads

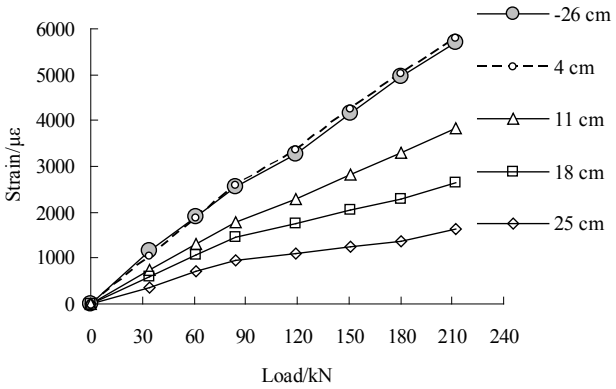

Figure 8. Load-strain curves at different anchor depths

Where, P is the tensile load undertaken at the loading end of anchor bolt; r is the diameter of bolt; z is the depth of the location of bolt; a is the parameter related to the elastricity modulus, poisson ratio of surrounding mass and the elastricity modulus of anchor bolt. Using this model to fit the test data can obtain the parameter a = -21.10.

Figure 9 shows that the difference between the test curves and model curves are little and therefore, this model can be used to simulate the test process reflecting the relationship between the axial force and the anchorage depth.

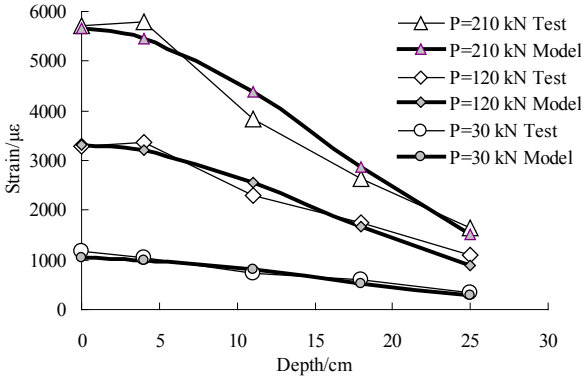

Figure 9. Strain-depth curves of model and test results

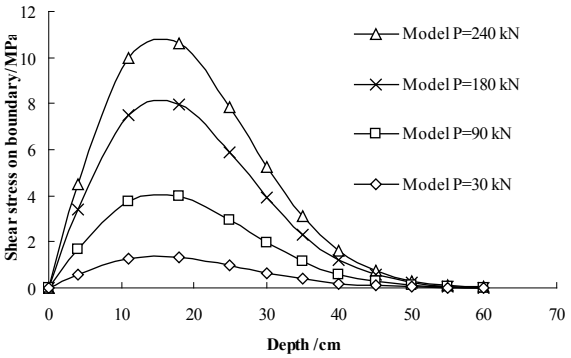

Figure 10. Variation of shear stress on GFRP bar surface

Figure 10 presents the relationship between shear stress and depth inside concrete under different loading level on the boundary of GFRP bar, which is obtained from the equation (5) based on the parameter a value.

According to the equation (5), it can be found that:

$$\text{When, } \frac{\mathrm{d}\tau}{\mathrm{d}z} = 0,$$

$$Z_{\tau_{\max}} = \sqrt{\frac{-1}{2a}} \tag{6}$$

Where, $Z_{\tau_{\max}}$ is the depth at which the maximum value of shear stress was created on the boundary between the GFRP bar and concrete.

According to the equation (6), the $Z_{\tau_{max}}$ is 15.4 cm. When the loading level is 240 kN, the τ_{max} is 10.92 MPa, and the average shear stress on the boundary is 7.85 MPa. Table 4 lists the calculation results of shear stress on the boundary of bolt.

It should be noticed that the maximum bond stress did not occur at the point close to the concrete cube edge of loading side. This may result from the slightly different elasticity modulus between GFRP bar and concrete.

Comparing the test results to the model results, it can be found that the test result of ultimate bond strength 9.24 MPa is larger than the model average shear stress 7.85 MPa, and smaller than the maximum value of model shear stress10.92 MPa. This relationship between them is reasonable. The model average shear stress is a little conservative for predicting the real bond strength of GFRP bar in concrete of an enginering construction.

Table 4. Model calculation results of shear stress changing with depth

Depth/cm	Shear stress on boundary /MPa				
	P = 30 kN	P = 90 kN	P = 120 kN	P = 180 kN	P = 240 kN
4.0	0.57	1.70	2.26	3.39	4.52
11.0	1.25	3.74	4.98	7.48	9.97
15.4	1.37	4.10	5.46	8.19	10.92
18.0	1.33	3.99	5.31	7.97	10.63
25.0	0.98	2.93	3.91	5.87	7.82
30.0	0.66	1.97	2.63	3.94	5.25

Appropriate Thickness of GFRP Anchor Bolt Frame Beam

Figure 10 also shows that the interface stress decreases to approach zero at the depth z_0 60 cm of frame beam. The thickness 30 cm of frame beam can not grouted GFRP bolt entirely, the shear stress in the bolt still exists at the edge of beam. In another words, all parts in the length 30 cm of bolt are effective for frame beam anchorage.

The equation (7) was defined to refelct the relationship between the total shear stress on bolt surface along the anchorage length of bolt and the thickness of frame beam:

$$S_z = \int_0^z \tau \mathrm{d}z = \int_0^z -\frac{azP}{\pi r}\exp(az^2)\mathrm{d}z = \frac{P}{2\pi r}[1-\exp(az^2)] \tag{7}$$

Where, S_z is the area of the shear stress distribution along anchorage length of bolt; z is the depth inside concrete.

The total shear stress is equal to the total load undertaken by anchor bolt. According to equation (7), the relationship between the total load on bolt at a certain anchorage depth z and that at the whole anchorage depth z_0 can be expressed as:

$$\frac{P_z}{P_{z_0}} = \frac{S_z}{S_{z_0}} = \frac{1-\exp(a\cdot z^2)}{1-\exp(a\cdot z_0^2)} \tag{8}$$

The equation (8) shows that the total load ratio of bolt is not related to loading level but only related to the anchorage depth. Relationships of load ratio and anchor length ratio with anchor length were presented in Figure 11.

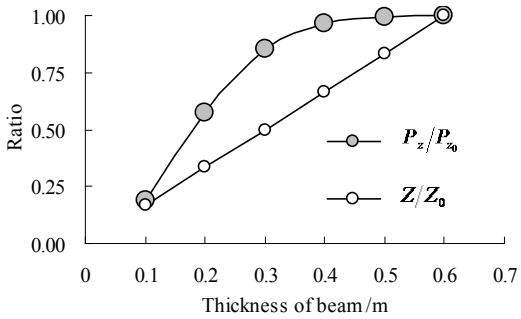

Figure 11. Relationships of load ratio and anchor length ratio with anchor length

From Figure 11, it can be seen that when the thickness of frame beam is 0.3 m the undertaken load of bolt reaches 85% of that of bolt anchored entirely with the thickness of 0.6 m, and this depth corresponds to the

anchoreage length ratio of 50%. When the thickness of frame beam is 0.4 m the ratio would be 97% corresponding to the anchoreage length ratio of 67%. Sum above, it can be found that when tht thickness of frame beam is more than 30 cm the increaseing rate of load in bolt becomes quite small with the anchorage length displayed in the Figure 11. Therefore, the appropriate thickness of frame beam for anchor bolt strucure should be 30 - 40 cm.

Bond Behavior of GFRP Bolt to Concrete under the Sustained Loading

Each phase loading was applied on the specimen for about 10 minutes. The data of strain and load in bolt were collected once a second. During each loading phase, the loading method for specimen is to keep a constant displacement for the test device by moving piston a certain space out of the hollow jack. During test the load can decreases a little gradually because of the stress relaxing in bolt. This loading procedure is similar to the real situation of prestressed anchor bolt working in a reinforcement structure of an civil construction.

Figure 12 displays strain-time curves at different anchor depths under the loads of 60 and 210 kN. In order to compare them, the vertical ordinates in figures of strain - time curve were drawn in the same scale.

For the situation of one load level, comparing the shape of curves at different location shows that the location of bolt nearer to the loading end has the bigger strain. In addition, it is also found that different location has different strain developing trend. For instance, the strain shows the whole decreasing trend near the loading end, while for the other end, it shows the whole increasing trend, as shown in Figure 12 (a) - (d).

The strain at different location in bolt can adjust automaticly during the load application. The part of bolt at small depth decreases its tensile strain to reduce the undertaking load, in contrary the part of bolt at larger depth increases its tensile strain to share the load transfered. Even though the total load on bolt is almost constant, the load distribution in the bolt changes significantly during the load maintaining.

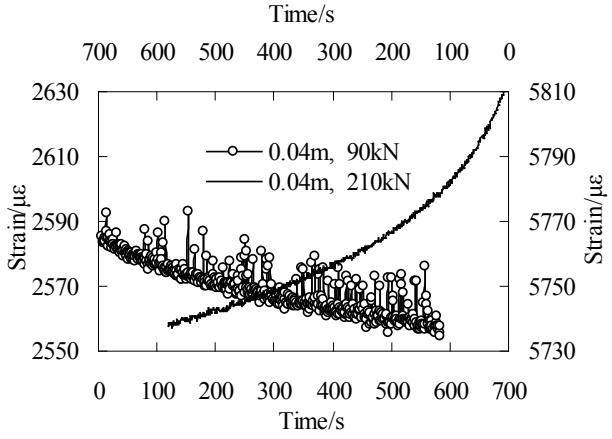

(a) Anchorage depth 0.04 m

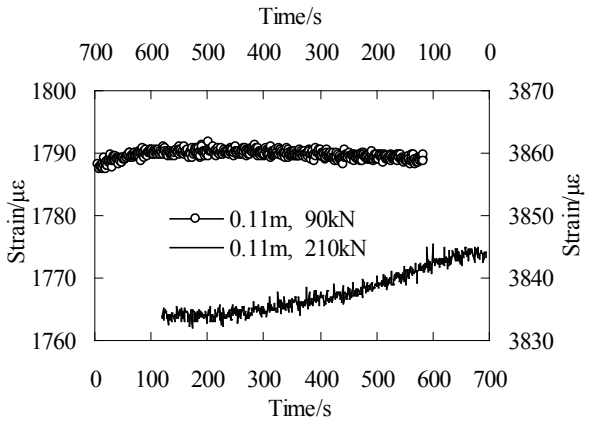

(b) Anchorage depth 0.11 m

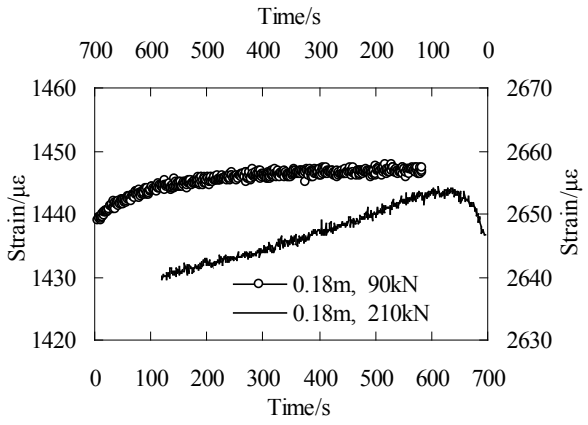

(c) Anchorage depth 0.18 m

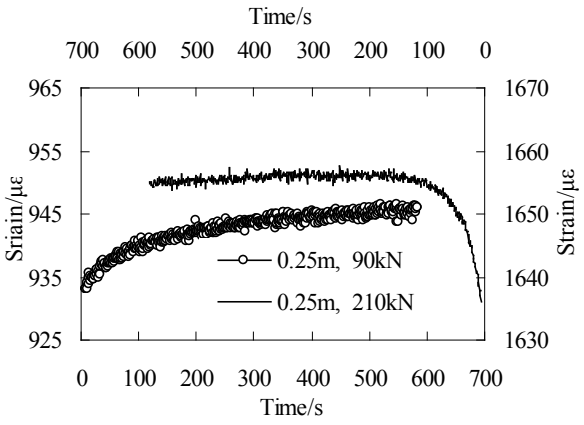

(d) Anchorage depth 0.25 m

Figure 12. Strain-time curves at different anchor depths under the load of 60 and 210 kN

For the situation of one location, comparing the shape of curves under different load level shows that the strain of bolt might show different trend. For instance, it can be seen in Figure 12 (c) that the curve of 90 kN displays the whole increasing trend and the curve of 210 kN displays the increasing trend at the beginning then change to decreasing trend.

Under the smaller load phase, the strain in bolt might be not yet to reach the peak value, which means this location of bolt can share more load again. Under the larger load phase, the strain might be decreasing, which means this location had experienced the peak load.

All of above phenomenons reveal that the shear stress of all points in the bolt was varing from zero to the peak with time during the prestress maintaining until the balance of strain distribution arriving. Therefore, the bond failure shoud be limited to take place at the point of loading end of bolt to prevent the failure from developing into the deeper position of mass.

Sum above, the shear stress distribution adjusting again of bolt should be caused by the bond behavior degradation btween bolt and mass. In addition, when loaded continuously, the bond between bolt and mass will degrade and the degradation will propagate to the deeper with time. The greater the load is applied, the deeper depth is extended to and the faster degradation proceeds. Therefore, the effect of bond behavior deterioration should be considered when deciding the magnitude of prestress for anchor bolt structur**.**

CONCLUSIONS

The objectives of this research program are to determine the optimum thickness of frame beam gripping the larger diameter GFRP bolt. One test model of GFRP bolt anchored in concrete cube was conducted on the bond behavior of interface between GFRP bolt and concrete; and ultimate pullout force under scheduled load simulated to the actual processes of prestressed anchor bolt structure is also investigated. Based on the experimental results and analytical studies on sand-coated GFRP bolt frame beam model under the described test conditions, the following conclusions can be drawn:

(1) For the large diameter sand-coated GFRP bolt (26.17mm) casted in concrete directly, the ultimate bond strength was 9.24 MPa which is much larger than the code bond strength value 2.7 MPa of the ribbed steel bar.

(2) For the situation of this test, the maximum bond stress at interface between GFRP bolt and concrete did not occur at the point close to the edge of concrete. The appropriate thickness of frame beam gripping GFRP bolt should be 30 - 40 cm.

(3) Sustained load can make the bond behavior deteriorate with time. For prestressed GFRP anchor bolt structure, more attention should be paid to the bond behavior deterioration at interface in the future, because it can significantly affect the durability of frame beam gripping function and the magnitude of prestressed load.

ACKNOWLEDGMENTS

The writers wish to express their gratitude and sincere appreciation for the financial support received from the government of Guangdong province and Ministry of education of China (Project No. 2009B09060011). The help received from the technical staff of the Rock and Soil Mechanics Laboratory in the college of civil and transportation engineering at the Hohai University is also acknowledged.

REFERENCES

Alsayed, S., Al-Salloum, Y., Almusallam, T., El-Gamal, S. and Aqel, M. (2012). “Performance of glass fiber reinforced polymer bars under elevated temperatures”, *Composites*: Part B, 43 (5), 2265-2271.

Alves, J., El-Ragaby, A. and El-Salakawy, E. (2011). “Durability of GFRP Bars’ Bond to Concrete under Different Loading and Environmental Conditions”, *Journal of Composites for Construction*, 15(3), 249-262.

Benmokrane, B., Tighiouart, B. and Chaallal, O. (1996). “Bond strength and load distribution of composite GFRP reinforcing bars in concrete”, *ACI Mater. J*., 93(3), 246-253.

Chen, Y., Davalos, J.F., Ray, I. and Kim, H.-Y. (2007). “Accelerated aging tests for valuations of durability performance of FRP reinforcing bars for concrete structures”, *Composite Structures*, 78 (3), 101-111 .

Chu, W. and Karbhari, V.M. (2005). “Effect of water sorption on performance of pultruded e-glass/vinylester composites”, *J. Mater. Civ. Eng*., 17(1), 63-71.

Kamal, A.S.M. and Boulfiza, M. (2011). “Durability of GFRP rebars in simulated concrete solutions under accelerated aging conditions”, *Journal of Composites for Construction*, 15(4), 473-481.

Karbhari, V.M., Chin, J.W., Hunston, D., Benmokrane, T., Juska, R., Morgan, R., Lesko, J.J., Sorathia, U. and Reynaud, D. (2003). “Durability Gap analysis for fibre reinforced polymer composites in civil infrastructure”, *J. Compos. Constr.*, 7(3), 238-241.

Koch, G.H., Brongers, M.P.H., Thomson, N.G., Virmanio, Y.P. and Payer, J.H. (2005). “Cost of corrosion in the United States”, *Handbook of Environmental Degradation of Materials*, M. Kutz, ed., William Andrew Publishing, Norwich, NY.

Li, G.-W., Ni, C., Pei, H.-F., Ge, W.-M., Ng, C.W.W. (2013). “Stress relaxation of grouted entirely large diameter B-GFRP soil nail”, *China Ocean Eng.*, 27(4), 495 – 508.

Masmoudi, R., Masmoudi, A., Ouezdou, M.B. and Daoud, A. (2011). “Long-term bond performance of GFRP bars in concrete under temperature ranging from 20 ℃ to 80 ℃”, *Construction and Building Materials*, 25 (2) 486-493.

Ministry of Construction China (2002). *Technical Code for Building Slope Engineering* (GB50330-2002), pp:35 (in Chinese)).

Nanni, A., Al-Zaharani, M.M., Al-Dulaijan, S.U., Bakis, C.E. and Boothby, T.E. (1995). “Bond of FRP reinforcement to concrete-Experimental results”, *Proc., 2nd Int. RILEM Symposium on Nonmetallic FRP Reinforcement for Concrete Structures* (FRPRCS-2), L. Taerwe, ed., E&FN Spon, Ghent, Belgium, 135-145.

Nkurunziza, G., Debaiky, A., Cousin, P. and Benmokrane, B. (2005). “Durability of GFRP bars: A critical review of the literature”, *Prog. Struct. Engng Mater*., 7(4), 194-209.

You, C. (2000). “Mechanical analysis of wholly grouted anchor”, *Chinese Journal of Rock Mechanics and Engineering*, 19(3), 399-341, (in Chinese).

Zhang, BR., Benmokrane, B., Chennouf, A., Mukhopadhyaya, P., and El-Safty, A. (2001). “Tensile behavior of frp tendons for prestressed ground anchors”, *Journal of Composites for Construction*, 5(2), 85-9.

Zeng, X.M., et al. (2004). “Research on safety and durability of bolt and cable-supported structures”, *Chinese Journal of Rock Mechanics and Engineering*, 23(13), 2235-2242.

Zhou, J.K., Chen, X.D. and Chen, S.X. (2011). “Durability and service life prediction of GFRP bars embedded in concrete under acid environment”, *Nuclear Engineering and Design*, 241(10), 4095- 4102.

Zhu, H.H., Yin, J.H., Yeung, A.T. and Jin, W. (2011). “Field pullout testing and performance evaluation of GFRP soil nails”, *Journal of Geotechnical and Geoenvironmental Engineering*, ASCE, 137(7), 633-641.